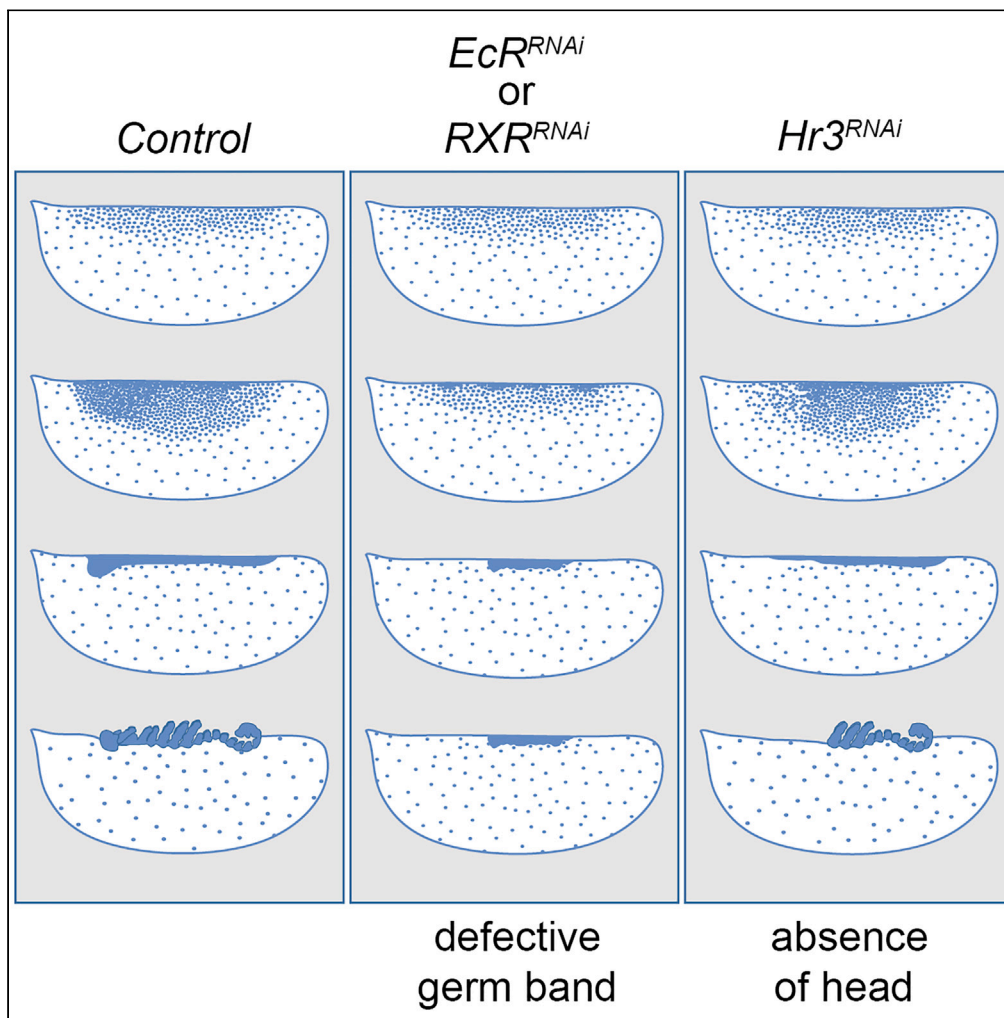


## Article

Nuclear receptors EcR-A/RXR and HR3 control early embryogenesis in the short-germ hemimetabolous insect *Blattella germanica*

Josefa Cruz, Oscar Maestro, Xavier Franch-Marro, David Martín

josefa.cruz@ibe.upf-csic.es (J.C.)  
david.martin@ibe.upf-csic.es (D.M.)

**Highlights**

The Ecdysone receptor heterodimer is required for germband formation

EcR-A/RXR induces the early expression of nuclear receptors E75-A, HR3-A, and FTZ-F1

Nuclear receptor HR3 is required for the formation of the embryo cephalic region

Germband formation is the first ecdysone-dependent transition in *Blattella germanica*

## Article

Nuclear receptors EcR-A/RXR and HR3 control early embryogenesis in the short-germ hemimetabolous insect *Blattella germanica*Josefa Cruz,<sup>1,2,\*</sup> Oscar Maestro,<sup>1</sup> Xavier Franch-Marro,<sup>1</sup> and David Martín<sup>1,\*</sup>

## SUMMARY

The role of steroid hormone signaling during insect post-embryonic development has been extensively characterized. However, its function during embryonic development is less understood, particularly in short-germ band hemimetabolous insects. To solve this, we have used *Blattella germanica* to analyze the embryonic functions of the heterodimeric ecdysone receptor, BgEcR-A and BgRXR. Here, we show that both transcripts are present from the beginning of embryogenesis, and that are required for proper germband formation. We also show that they regulate an early induction of a stereotypical cascade of nuclear receptors. Notably, we found that one of these, *BgHR3*, controls the formation of the cephalic region of the germband. Finally, spatial expression of two other receptors, *BgE75-A* and *BgFTZ-F1*, suggest their involvement in the formation of the nervous system and in germband segmentation, respectively. In summary, our results highlight the critical roles of ecdysone-signaling during early embryogenesis in short-germ band hemimetabolous insects.

## INTRODUCTION

Steroid hormones play a central role in reproduction, metabolism, and development in higher organisms. In insects, they also regulate major developmental transitions, an effect that is mediated by periodic pulses of the steroid hormone 20-hydroxyecdysone (hereafter referred to as ecdysone). During post-embryonic development, these pulses promote successive molting, hence accommodating the progressive growth of the immature insect. Then, at the end of the juvenile development, a specific ecdysone burst promotes the metamorphic transition to adulthood either directly (hemimetabolous insects) or through the intermediate pupal stage (holometabolous insects).<sup>1,2</sup>

From a molecular perspective, ecdysone exerts its regulatory function upon binding to the Ecdysone receptor (EcR), a member of the nuclear receptor superfamily, which heterodimerizes with another nuclear receptor, the retinoid X receptor (RXR)-ortholog ultraspiracle (USP).<sup>3–7</sup> This heterodimer elicits cascades of gene expression, including transcription factors *Broad-complex*, *E74*, *E93*, and a number of nuclear receptors, such as *E75*, *HR3*, and *FTZ-F1*. This core set of transcription factors mediates and amplifies the hormonal signal during each developmental transition of the insect (Cheatle Jarvela and Pick, 2017; Thummel, 1995; King-Jones and Thummel, 2005; Martín, 2010; Ou and King-Jones, 2013; Riddiford et al., 2000).<sup>4,8–12</sup>

In contrast to the well-characterized role of ecdysone signaling during post-embryonic transitions in hemimetabolous insects, its function during embryonic development has been studied mainly in holometabolous insects, particularly in the fruit fly *Drosophila melanogaster*. Embryogenesis in *D. melanogaster* follows a long-germ band mode of development, in which almost the totality of cells of the blastoderm forms the embryo proper and all segments are formed simultaneously.<sup>13</sup> From an endocrine perspective, *D. melanogaster* embryogenesis presents a single high titer pulse during mid-embryogenesis (25–50% of embryonic development), which correlates with three critical morphogenetic events: germband retraction, dorsal closure and head involution.<sup>14,15</sup> Consistent with the timing of this ecdysone pulse, disruption of embryonic ecdysone signaling by expressing a dominant-negative EcR protein or by reducing the titer of ecdysone produces a block in the retraction of the germband and the involution of the head.<sup>16</sup> Similarly, embryos derived from germline clones with *usp* mutant allele show the same phenotype,<sup>17</sup> which is indicative of EcR and USP acting together at mid-embryogenesis to promote two major

<sup>1</sup>Institute of Evolutionary Biology (CSIC-Universitat Pompeu Fabra), Passeig Marítim de la Barceloneta 37-49, 08003 Barcelona, Spain

<sup>2</sup>Lead contact

\*Correspondence: josefa.cruz@ibe.upf-csic.es (J.C.), david.martin@ibe.upf-csic.es (D.M.)

<https://doi.org/10.1016/j.isci.2023.106548>



morphogenetic events that shape the larval body plan. In addition to this function, ecdysone signaling is also required during mid-late embryogenesis for proper deposition of the cuticle in ectodermal tissues, such as the tracheal system and the epidermis.<sup>18</sup> Ecdysone signaling, therefore, acts as a central regulator of developmental transitions in both, embryonic and post-embryonic periods in long-germ band holometabolous insects.

Contrary to the detailed information from *D. melanogaster*, very little is known about ecdysone signaling in the embryogenesis of hemimetabolous species. To gain insight into this question, here we analyzed the presence and role of ecdysone signaling in the embryogenesis of the hemimetabolous German cockroach *B. germanica*. Embryogenesis of *B. germanica* has been previously described, including the classification of different stages based on morphological characteristics of the embryo (Figure S1A),<sup>19–21</sup> and differs from that of *D. melanogaster* in some critical features. First, *B. germanica* follows a short-germ band type of embryonic development, in which only the most anterior cephalic and thoracic segments of the embryo are specified during the early syncytial blastoderm stage. The abdominal segments are then sequentially added during the germband elongation from a posteriorly located undifferentiated growth zone (GZ) of proliferating cells.<sup>13</sup> Second, two clear ecdysone pulses are present during *B. germanica* embryogenesis: the first at day 6 after ootheca formation (AOF) (30–40% of embryonic development (ED)), which is associated with dorsal closure, and the second one between days 12 and 14 AOF (65–90% ED), correlating with the deposition of the first instar nymphal cuticle (Figure S1B).<sup>22</sup>

Despite the presence of these two ecdysone bursts, we unexpectedly observed in previous studies that the earliest expression of ecdysone-dependent genes in *B. germanica* embryogenesis occurred around 36–48 h AOF (8–12% of embryonic development (ED)),<sup>22,23</sup> which is significantly before the mid- and late ecdysone peaks. This observation suggests that, in contrast to long-germ band *D. melanogaster*, ecdysone signaling might be necessary during the very first stages of *B. germanica* embryogenesis. In the present study, we have confirmed this suggestion by showing that mRNAs for BgEcR-A and BgRXR, which conform the heterodimeric ecdysone receptor of *B. germanica*,<sup>24,25</sup> are present from the beginning of embryogenesis and that are required during the blastoderm stage for an early activation of the stereotypical ecdysone-dependent cascade of nuclear receptors and the proper formation of the germband. Moreover, we have demonstrated that one of these nuclear receptors, BgHR3, specifically controls the formation and development of the cephalic region of the germband and that another two nuclear receptors, BgE75A and BgFTZ-F1, might be involved in the formation of the nervous system and the regulation of germband segmentation, respectively. Altogether, these results suggest that ecdysone signaling is critical during the very early stages of the short-germ hemimetabolous *B. germanica*, and reveal germband formation as the first developmental transition in the life cycle of this type of insect that depends on the presence of the ecdysone receptor, BgEcR-A and BgRXR.

## RESULTS

### Early embryonic development in *B. germanica*

To test the possible role of ecdysone signaling during the first stages of *B. germanica* embryogenesis, we first established a detailed morphological description of the cellular dynamics during the first 60 h of embryogenesis (Figure 1A). After fertilization and fusion of the male and female pronuclei near the center of the egg, energid proliferation and migration to the periphery of the egg begins. As a result, an array of nuclei first appeared on the ventral surface of the egg at about 12 h AOF (3% ED), and then to the most dorsal part by 18 h AOF (4.4% ED). By 24 h AOF (6% ED), a uniform distribution of energids throughout the surface of the egg was achieved. Later, between 36 and 54 h AOF (8–13% ED), the energids located at the ventral part (0–50% of the egg width) intensively proliferate and started to migrate toward the most ventral part of the egg, where they aggregated to form a bipartite germ anlage. Finally, at 60 h AOF (15% ED), the bipartite germ anlage started to merge at the most ventral part of the egg to form the germband (Figure 1A). At this point, the protocephalon (anterior head region) and the thorax were detectable in the germband, as several stripes from the head segments to the T2 segment were revealed by immunostaining with the pan-segmental marker Engrailed (En) (Figure 1B). During early and late germband elongation, 62–78 h AOF (15.1–19% ED), additional stripes of En appeared sequentially from the posterior GZ to form the abdominal part of the embryo (Figure 1B). On the other hand, cells located outside the embryonic primordium become polyploid giving rise to an extraembryonic membrane, the serosa (Figure S2).

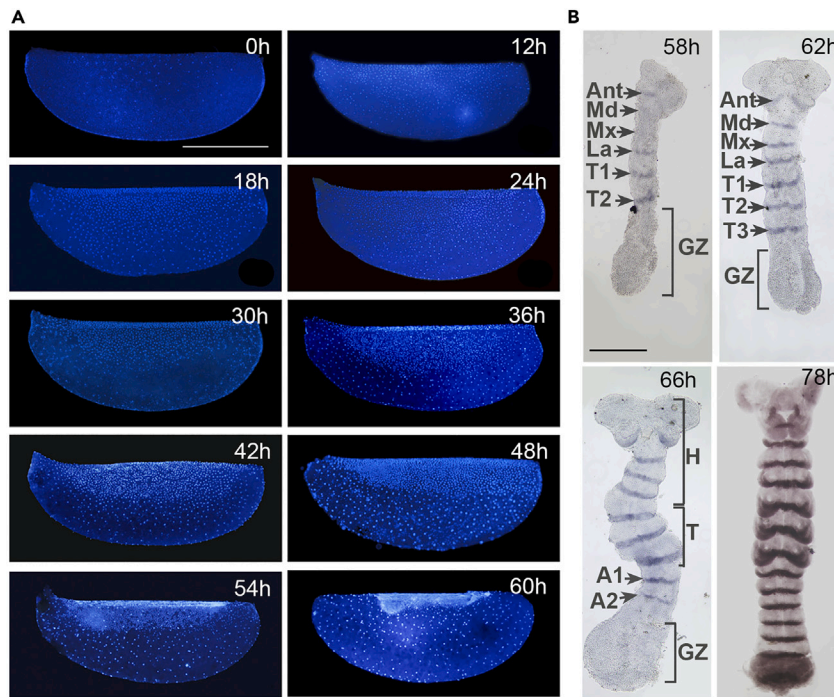


**Figure 1. Cellular dynamics during early *B. germanica* embryogenesis**

(A) Lateral views of DAPI-stained whole eggs during the first 60 h of embryogenesis. Time after ootheca formation (AOF) is shown by white numbers. Anterior toward the left and ventral toward the top of the eggs. After fertilization energids proliferate and migrate to the periphery of the egg (0 h AOF), first arriving at the ventral surface around 12 h AOF, and to the dorsal surface at 18 h AOF. A uniform distribution of energids is observed by 24 h AOF. Energids at the ventral part proliferate and migrate toward the most ventral part of the egg, aggregating to form a bipartite germ anlage (36–54 h AOF). The bipartite germ anlage merges at the most ventral part of the egg to form the germband by 60 h AOF.

(B) Expression of the segmental marker Engrailed during germband formation (58–78 h AOF), showing progressive occurrence of segments in the thoracic and abdominal regions. Head (H); antennal (Ant), mandibular (Md), maxillar (Mx) and labial (La), thoracic (T; T1–T3) and abdominal (A1–A7) segments are indicated; GZ: proliferative growth zone. Scale: 1 mm in A; 250  $\mu$ m in B.

### Early occurrence of ecdysone signaling in *B. germanica* embryogenesis

To establish a correlation between the morphological changes described above and the presence of ecdysone signaling, we examined the expression levels of the heterodimeric ecdysone receptor of *B. germanica*, BgEcr-A and BgRXR, during the period studied. As shown in Figure 2A, transcripts for BgEcr-A and BgRXR receptors were maternally supplied and were present throughout the early stages of embryogenesis. Of the two BgRXR mRNAs described in *B. germanica*,<sup>22</sup> only BgRXR-L transcript was constantly present as BgRXR-S was not detected until 36 h AOF. Remarkably, *in situ* hybridization revealed that at the late blastoderm stage the mRNAs from both transcripts were detected surrounding the nuclei of cells that were actively proliferating and migrating to form the germ anlage (Figures 2B and 2C).

Next, we analyzed the expression of the nuclear receptor genes BgE75-A, BgHR3-A, and BgFTZ-F1, which form a highly stereotypical hierarchy that is activated by ecdysone during each post-embryonic transition of *B. germanica*.<sup>23,26–29</sup> As Figure 2A shows, BgE75-A, BgHR3-A, and BgFTZ-F1 showed a transient burst of expression beginning at 36–48 h AOF, which correlates with the maternal-to-zygotic transition,<sup>30</sup> and ending at 60 h AOF (Figure 2A). Expression of the ecdysone-independent nuclear receptor BgSeven-up (BgSvp), and ribosomal proteins BgRib-S16 and BgRib-L22 was also induced by 36–48 h AOF but, in contrast to the ecdysone-dependent genes, their expression was maintained by 72 h AOF (Figure 2A). Remarkably, this early transient activation of ecdysone-dependent genes was not correlated with any detectable pulse of ecdysteroids as the levels of these hormones remained constant during the first 72 h of embryogenesis (Figure 2A). Taken together, these results show that in *B. germanica* embryogenesis ecdysone signaling activation occurs as early as 36–60 h AOF (8–12% ED), coinciding with the

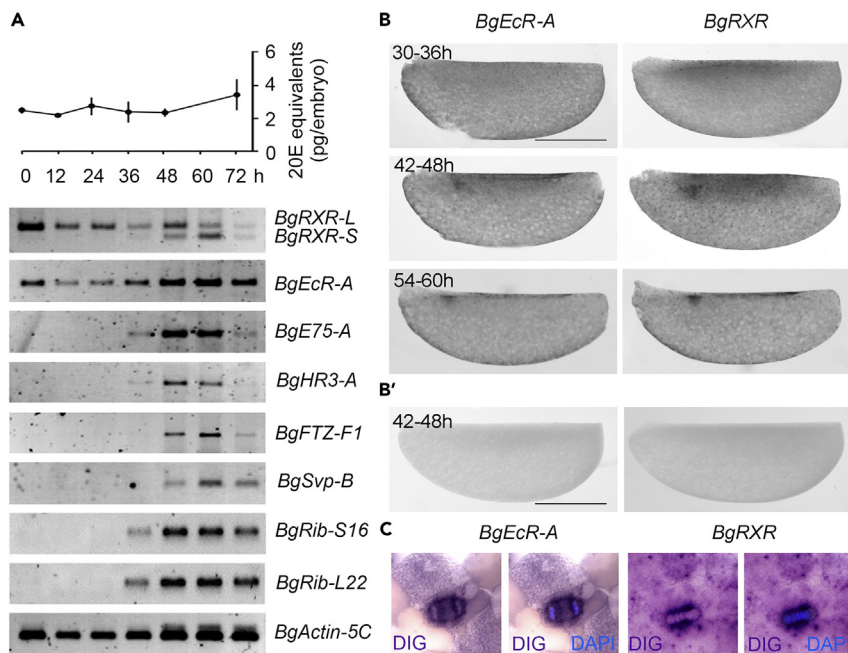


**Figure 2. The ecdysone-dependent transcriptional cascade occurs during the early embryogenesis of *B. germanica***

(A) Temporal profiles of transcription factor gene expression during early embryo development (0–60 h AOF). Equal amounts of staged embryos were analyzed by RT-PCR. *BgActin5C* levels were used as a reference. The blots are representative of five replicates. Ecdysteroid levels during the same period were measured by ELISA (upper part). Error bars indicate the SEM.

(B) Expression pattern of *BgEcR-A* and *BgRXR* between 30 and 60 h AOF revealed by *in situ* hybridization. Expression of both receptors is detected in cells that proliferate and migrate to form the germ anlage.

(B') As a control, embryos hybridized with sense *BgEcR-A* and *BgRXR* probes showed no staining.

(C) *BgEcR-A* and *BgRXR* transcripts are localized around the nucleus of blastoderm cells. *in situ* hybridizations are merged with nuclear staining by DAPI. Scale: 1 mm.

maternal-to-zygotic transition and the onset of the proliferation and migration of the cells that will form the germband at the most ventral part of the embryo.

### BgEcR-A and BgRXR requirement during early embryogenesis

To investigate the role of early ecdysone signaling, we use parental RNAi (pRNAi) to silence the expression of *BgEcR-A* and *BgRXR* during this period. To this aim, 5-day-old adult females of *B. germanica* were injected with *dsRNAs* encompassing the LBDs of both nuclear receptors (*BgEcRi* and *BgRXRi* animals). Specimens injected with *dsMock* were used as negative controls (*Control* animals). Under these conditions, *BgEcR-A* and *BgRXR* mRNA levels showed a marked and specific reduction at the beginning of embryogenesis (Figure S3A). Importantly, the removal of these receptors did not affect the proper formation of oothecae nor the levels of maternally deposited ecdysteroids (Figure S3B and Table S1).

Aside from 2% of unfertilized eggs, the great majority of *BgEcRi* and *BgRXRi* embryos displayed similar strong phenotypes (Figure 3A and Table S1). As revealed by DAPI staining, they showed normal embryonic development up to 30–36 h AOF. However, from that stage, knockdown embryos presented a clear decrease in the number of cells destined to form the germinal band (Figure 3A). The reduction in cell number was not due to increase cell death (Figure S4), but to impairment in cell proliferation as revealed by immunocytochemistry using anti-PH3 (Figures 3C and 3D). Despite the problems in proliferation, cells migrated correctly toward the ventral side of embryo where they condensed to form a much smaller germband that did not progress any further (Figures 3A, 3A', and 3B). In contrast, the absence of *BgEcR-A* and *BgRXR* did not cause the loss of the serosal cell fate as revealed by the normal density, spacing, and ploidy levels of the serosal cells (Figures 3A' and 3E), consistent with the absence of *BgEcR-A* and *BgRXR* mRNAs in these cells.



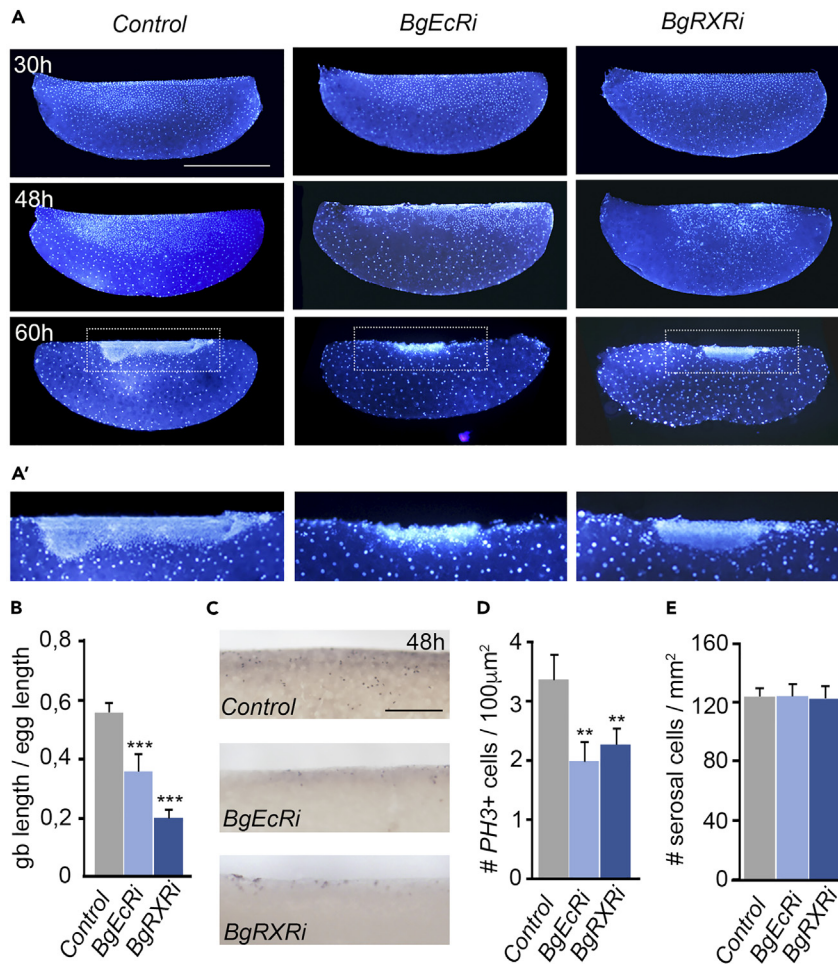


**Figure 3. Functions of BgEcR-A and BgRXR in early embryos of *B. germanica***

(A) Development of early embryos after pRNAi of BgEcR-A (*BgEcRi*) and BgRXR (*BgRXRi*). Lateral views of DAPI-stained Control (left row), *BgEcRi* (middle row), and *BgRXRi* (right row) whole eggs. Time after ootheca formation (AOF) is shown by white numbers. Anterior toward the left and ventral toward the top of the eggs. Knockdown embryos presented normal embryonic development until 30–36 h AOF, but a significant decrease in the number of cells fated to become the germinal band from this point. Although the cells migrate toward the ventral part they form a significantly smaller germband that stop developing.

(A') High magnification of the rectangles in A showing the reduced germ bands of *BgEcRi* and *BgRXRi* embryos.

(B) Graph showing the reduction of the germband anlage in *BgEcRi* and *BgRXRi* compare to the Control.

(C) BgEcR-A and BgRXR promote cell proliferation during early embryo development. Control, *BgEcRi*, and *BgRXRi* embryos were stained with PH3 to reveal cell proliferation at 48h AOF.

(D) Graph showing the average number of PH3-positive cells in Control, *BgEcRi*, and *BgRXRi* embryos.

(E) Graph showing no differences in the number of serosal cells in *BgEcRi* and *BgRXRi* embryos compared to the Control.

Error bars indicate the SEM. Asterisks indicate differences statistically significant in B, D, and E as follows:  $p \leq 0.005$  (\*\*),  $p \leq 0.0005$  (\*\*\*), ( $n = 8-14$  in B and D and  $n = 6-12$  in E). Scale bars: 1 mm in A; 200  $\mu\text{m}$  in C.

Next, we analyzed if the presence of BgEcR-A and BgRXR was required for the timely activation of ecdysone-dependent genes at 36–60 h AOF. To this aim, RNA samples from staged *BgEcRi* and *BgRXRi* embryos were analyzed by qRT-PCR. As Figure 4 show, mRNA levels of ecdysone-inducible genes *BgE75A*, *BgHR3*, and *BgFTZ-F1* were significantly reduced in *BgEcRi* and *BgRXRi* embryos, whereas those of the ecdysone-independent gene *BgSvp-B* were not affected. Taken together, our results demonstrate that BgEcR-A and BgRXR are required during early embryogenesis in *B. germanica* for the early deployment of the stereotypical cascade of nuclear receptors as well as for the proliferation of the cells that eventually will form the germ anlage.

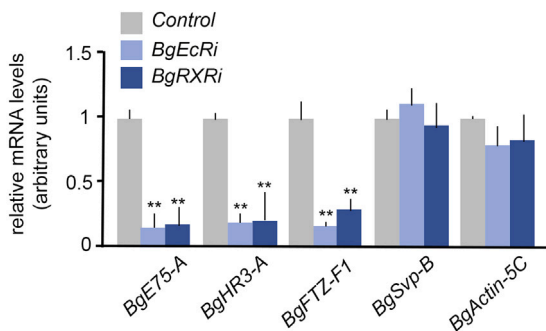


**Figure 4. Effect of *BgEcR-A* and *BgRXR* depletion on ecdysone-dependent gene expression in early embryos of *B. germanica***

Transcript levels of nuclear receptors *BgE75-A*, *BgHR3-A*, *BgFTZ-F1* and *BgSvpB* in Control, *BgEcRi*, and *BgRXRi* embryos at 48 h AOF, measured by qRT-PCR. Fold changes in each transcript level are relative to their expression in Control embryo, arbitrarily set to 1. Error bars indicate the SEM (n = 6–8). Asterisks indicate differences statistically significant compared to the control as follows: p ≤ 0.005 (\*\*).

### Expression patterns of *BgE75A*, *BgHR3* and *BgFTZ-F1* during embryogenesis

The temporal coincidence between the *BgEcRi* and *BgRXRi* phenotypes and the up-regulation of several nuclear receptor genes suggested that components of this ecdysone-dependent hierarchy might be involved in the formation and development of the germband. To examine this possibility, we first analyzed the spatial expression of *BgE75A*, *BgHR3-A*, and *BgFTZ-F1*, as they are functionally linked during post-embryonic development in *B. germanica* (Cruz et al., 2008; Mané-Padrós et al., 2008, 2010). *In situ* hybridization analysis revealed that *BgE75A* mRNA was detected in the blastoderm stage (36–48 h AOF) in cells that would give rise to the germband (Figure 5A, left panel). Later, as the germ anlagen condensed (54–60 h AOF), its expression became restricted to a region in the center of each head lobe and to two lateral stripes that likely represent the developing nervous system, including the brain and the ventral nerve cord (Figures 5B and 5B', left panels). Similarly, *BgHR3* mRNA was also detected in germband cells at the blastoderm stage (Figure 5A, middle panel), although its expression was later restricted only to the cephalic region (Figures 5B and 5B', middle panels). Finally, *BgFTZ-F1* presented a striped expression as the germband forms appearing from the mid-posterior half and persisting as the germband elongated (Figures 5A–5B', right panels, and 5C). Together, these results strongly suggest that these factors are involved in the formation and development of the germband during the early embryogenesis of *B. germanica*.

### *BgFTZ-F1* requirement in *B. germanica* oogenesis

The expression pattern of *BgFTZ-F1* in the GZ of the germband pointed to a putative role in the formation of the abdomen and the segmentation process. To analyze this possibility, we carried out the same pRNAi approach that we used previously. Unfortunately, pRNAi for *BgFTZ-F1* resulted in females that did not form any ootheca regardless of the age at which the *dsBgFTZ-F1* was injected into the female, which precluded the functional analysis of the embryonic role of this factor. To ascertain the reason for this effect, we studied the expression and function of *BgFTZ-F1* in the oogenesis of adult *B. germanica* females. *BgFTZ-F1* was expressed in the ovary throughout the adult stage, with a modest increase toward the end of the first gonadotrophic cycle at the choriogenic stage (Figure S5A). *BgFTZ-F1* transcripts were detected in the follicular cells that surround the basal oocyte as well as in the immature oocytes that precede the basal one, but were absent from the egg cell (Figure S5B). Administration of *dsBgFTZ-F1* in adult *B. germanica* females drastically reduced mRNA levels of *BgFTZ-F1* in 7-day-old ovaries (Figure S3C), and resulted in a complete block of the last steps of oogenesis. A detailed analysis revealed that follicular cells from basal oocytes of *dsBgFTZ-F1*-treated females failed to rearrange the actin filaments during choriogenesis, a process that is required for proper ovulation, resulting in a completely disorganized actin structure. The cells did not fuse at the final step of oogenesis and the follicular epithelium eventually degenerated, as evidenced by the irregular distribution and aberrant shape of their nuclei (Figures S5C and S5D). These results demonstrate that *BgFTZ-F1* is critical for *B. germanica* oogenesis.

### *BgHR3* requirement during embryonic development

In contrast to *BgFTZ-F1*, pRNAi for *BgHR3* (*BgHR3i* embryos) was effective in analyzing the role of this factor during early embryogenesis. Thus, the administration of *dsBgHR3* into 5-day-old adult females of *B. germanica* did not affect the formation of the ootheca and resulted in a clear decrease in embryonic *BgHR3* mRNA levels (Figure 3D). Notably, 27% of *BgHR3i* embryos showed impaired embryonic development (Table S2). Detailed quantification of the phenotypes indicated a graded variability within a

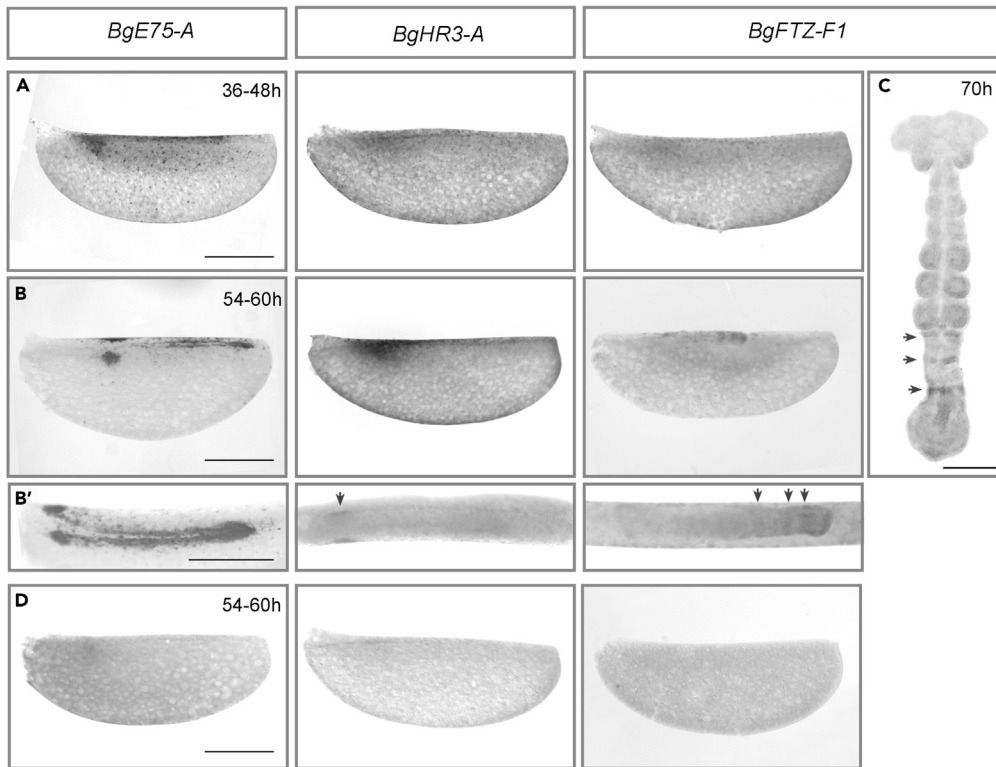


**Figure 5. Expression patterns of *B. germanica* BgE75-A, BgHR3, and BgFTZ-F1 in early embryos**

Expression patterns of BgE75 (left), BgHR3 (middle), and BgFTZ-F1 (right) during the formation of the germband at (A) 36–48 h and (B, B') 54–60 h AOF, revealed by *in situ* hybridization. Lateral views in A and B, and ventral view in B'. BgE75 is detected in the cephalic region and two lateral stripes of the germband, while the expression of BgHR3 is restricted to the cephalic region and BgFTZ-F1 transcript is detected in a striped expression pattern at the posterior part of the germband. (C) Striped pattern of BgFTZ-F1 transcripts persists as the germband elongates. (D) As a control, embryos hybridized with sense BgE75-A, BgHR3, and BgFTZ-F1 probes showed no staining. Scale bars: 1 mm in A–B' and D; 250  $\mu$ m in C.

requirement for anterior development, which was consistent with the expression of BgHR3 in the anterior part of the germband. We classified BgHR3i embryos according to the strength of the phenotype into two different classes (Table S2). In Class I embryos only the thoracic and abdominal segments formed, although the thoracic segments developed with some truncations. The anterior cephalic region was mostly formed by undifferentiated tissue, revealed by complete or near-complete loss of En staining (Figure 6). In Class II embryos only the most anterior cephalic segments, antennae, and mandible, were missing whereas the rest of the germband, including maxilla, labium, as well as all the thoracic and abdominal segments, developed properly (Figures 6A and 6B). The same phenotype was observed when a second dsRNA targeted to BgHR3 was used (Figure S6). Altogether, our results showed that ecdysone-dependent BgHR3 is specifically required for the proper development of the cephalic region during the early stages of *B. germanica* embryogenesis.

## DISCUSSION

In this study, we demonstrated that the formation and development of the germband is the earliest developmental transition in the hemimetabolous insect *B. germanica* that depends on the function of the ecdysone receptor, BgEcr-A and BgRXR. Our work shows that BgEcr-A and BgRXR are present from the beginning of embryogenesis and that they play a crucial role in controlling the first stages of embryonic development, particularly in the proliferation of the cells that will generate the germband. We also found that they are also required for the early deployment of the ecdysone-dependent gene cascade just at the maternal-to-zygotic transition. Finally, our findings also show that two ecdysone dependent genes, BgHR3 and BgFTZ-F1 have relevant roles in germband formation. Whereas BgHR3 controls the development of



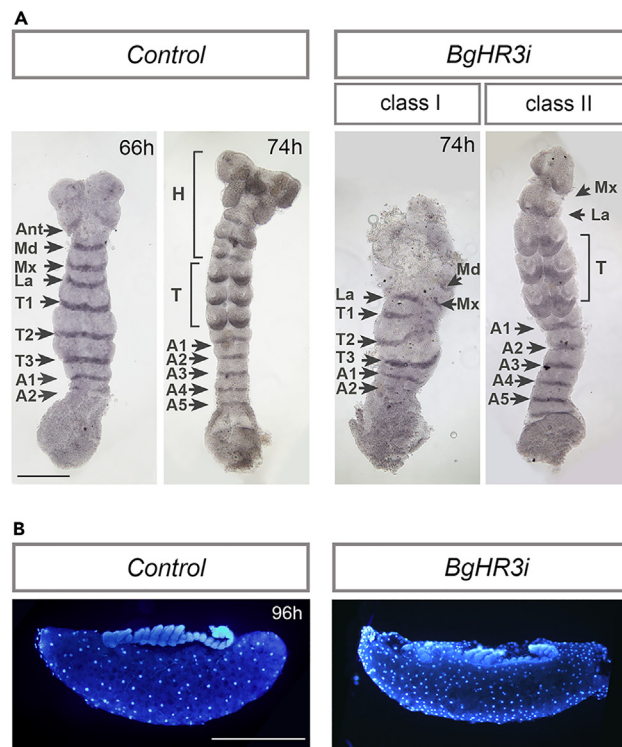


**Figure 6. Function of BgHR3 in early embryogenesis of *B. germanica***

(A) Development of the germband after pRNAi of *BgHR3* (*BgHR3i*) reveals a strong impairment in the formation and development of the cephalic segments revealed by the expression of the segmental marker *Engrailed*. The affectionation is stronger in class I *BgHR3i* germ bands compared to class II germ bands. Head (H); antennal (Ant), mandibular (Md), maxilar (Mx) and labial (La), thoracic (T), and abdominal (A1–A5) segments are indicated. Time after ootheca formation is shown in each panel.

(B) Lateral views of DAPI-stained *Control* (left panel) and *BgHR3i* (right panel) whole embryos 96h after ootheca formation. The *BgHR3i* panel is representative of a class II embryo showing the lack of the most anterior cephalic regions. Scale bars: 250  $\mu$ m in (A) and 1 mm in (B).

the cephalic region in the anterior region of the germband, *BgFTZ-F1* striped expression suggested a role in the segmentation of the germband.

### Early ecdysone-signaling requirement in *B. germanica* embryogenesis

Our results, along with previous studies, show that the ecdysone-dependent signaling cascade occurs at three different periods during *B. germanica* embryogenesis: (1) at 8–12% ED (this study); (2) at 30–40% ED, correlating with the dorsal closure and deposition of the pronymphal cuticle; and (3) at 65–90% ED, which might be related with the formation of the first nymphal instar structures and the deposition of the first instar nymphal cuticle.<sup>22,23</sup> The earliest period, characterized here, spanned a narrow window of time (36–60 h AOF) that starts at the maternal-to-zygotic transition and spans the formation of the germband. Remarkably, this period is characterized by the absence of a detectable ecdysteroid pulse, although significant amounts of ecdysteroids were still detected during the first 60 h of embryogenesis, suggesting that these hormones are maternally deposited, stored, and used for the early activation of the ecdysone signaling. A similar situation is found in *Bombyx mori* embryogenesis, where ecdysone is provided not simply by the *novo* synthesis but also by the dephosphorylation of maternally derived ecdysteroid conjugates.<sup>31–33</sup> Likewise, ecdysteroids required during mid-embryogenesis in *D. melanogaster* are also maternally deposited, stored as inactive conjugates in the yolk, and later converted into their active forms in an extraembryonic tissue, the amniosera.<sup>34,35</sup> However, although the source of ecdysteroids at the onset of embryogenesis is the same between short- and long-germ band insects, clear differences can be observed in the ecdysteroid profiles between both types of embryogenesis. Whereas several ecdysteroid pulses are present in short-germ band insects,<sup>36–38</sup> a single mid-embryonic peak is observed in long-germ band insects.<sup>14,39,40</sup>

Regarding the expression patterns of *BgEcR-A* and *BgRXR-L*, our results indicate that they are maternally supplied. Interestingly, *BgRXR-L* is the only isoform detected during the first 36 h AOF, which is consistent with this isoform being the only one expressed in the ovaries of *B. germanica* during the gonadotrophic cycle.<sup>22</sup> Maternal contribution to embryonic *EcR* and *USP* mRNAs has been also described in *D. melanogaster*.<sup>16,39</sup> Interestingly, at the blastoderm stage, *BgEcR-A* and *BgRXR* mRNAs were detected surrounding cells that were fated to become germband, whereas were absent in cells fated to form the serosa. Consistent with their spatial expression, *BgEcR-A* and *BgRXR* loss-of-function embryos displayed impaired cell proliferation that resulted in abnormal germ bands but did not affect serosal cell fate. The control of cell proliferation by ecdysone has already been observed in the post-embryonic development of *B. germanica*, particularly in the ovarian follicle and wing cells.<sup>23,41</sup> Likewise, ecdysone also controls cell proliferation in specific cell types in *D. melanogaster*. For example, the ecdysone pulse that induces the prepupal transition induces the proliferation of cells in the wing discs,<sup>41</sup> as well as of the abdominal histoblasts that make up the progenitor cells of the adult abdominal epidermis.<sup>42,43</sup> However, despite the fact that ecdysone controls cell proliferation in both types of insects, our pRNAi experiments show that the requirement for ecdysone signaling is very different between the embryogenesis of short- and long-germ band insects. While *BgEcR-A* and *BgRXR* are required at the onset of embryonic development to control germband formation, in *D. melanogaster* both receptors work together much later, in the middle of embryogenesis, to control critical morphogenetic movements, such as the retraction of the germband and the involution of the head, as well as for the morphogenesis of the different organs.<sup>16,17</sup> It seems plausible, then, that the evolution from short-germ band to long-germ band was favored by the loss of control by ecdysone signaling of the initial stages of embryogenesis. These differences, therefore, might reflect a key feature in the evolution of the different types of insect embryogenesis/development. Further studies using other short- and long-germ band insects will be required to confirm this hypothesis.

### **BgHR3 controls the formation of the cephalic region**

Our results demonstrate that the deployment of an ecdysone-dependent signaling cascade of hormone nuclear receptors at the maternal-to-zygotic transition is essential for germband formation. The early presence of members of such cascade seems to be a conserved feature of hemimetabolan embryogenesis as it has been also observed in the hemipteran *Oncopeltus fasciatus*.<sup>44,45</sup> It is important to note that this same cascade, including *E75A*, *HR3*, and *FTZ-F1*, is observed in all developmental transitions that are controlled by ecdysteroid pulses during the post-embryonic development of *B. germanica*.<sup>23,26–29</sup> Likewise, it was also found during *D. melanogaster* development, following the ecdysteroid pulses in mid-embryogenesis and between second to third larval instar and larval-pupal transitions.<sup>39</sup> These observations clearly indicate that this stereotypical hierarchy of ecdysone-dependent nuclear receptors acts as the temporal timer of critical developmental events throughout the life cycles of insects, and, reveal that the formation and progression of the germband is the earliest developmental transition in a short-germ band type of embryogenesis that is controlled by *BgEcR-A* and *BgRXR*.

In particular, our results have shown that nuclear receptor *BgHR3* is essential for the formation and development of the cephalic region of the germband. Interestingly, the predominant expression of *BgHR3* in the anterior region of the embryo during the blastoderm stage, before the germband is totally formed, suggests that the spatial specification of the head by *BgHR3* might precede the formation of the germband, a possibility that has been confirmed by the reduction or elimination of the anterior head region in *BgHR3i* embryos. Interestingly, the expression and function of the cephalic gap gene *orthodenticle* (*otd*) in short-germ band insects, such as the cricket *Gryllus bimaculatus* and the beetle *Tribolium castaneum*, are consistent with the fact that head specification takes place before the onset of the aggregation of the germ-anlage cells.<sup>46,47</sup> Therefore, our results together with previous ones, suggest that the specification of the head region in short-germ band embryos occurs at the cellularized blastoderm stage, prior to the formation of the germband, under the control of not only cephalic gap genes (*otd*) but also of ecdysone-dependent genes (*EcR*, *RXR*, *HR3*). Whether the activation of these genes occurs in parallel or is somehow interconnected requires further study.

### **BgFTZ-F1 likely controls embryo segmentation and is required for adult oogenesis**

Although pRNAi for *BgFTZ-F1* has failed to provide evidence for an embryonic role of this factor, clear spatial differences were observed for *BgHR3* and *BgFTZ-F1* expression. These differences strongly suggest non-overlapping functions of both receptors during early *B. germanica* embryogenesis, a situation that contrasts with that observed in post-embryonic development, where both factors overlap in regulating

the same developmental processes.<sup>26,27</sup> In contrast to the cephalic expression of *BgHR3*, the striped expression of *BgFTZ-F1* in the thorax and abdomen of germ bands points to a possible function in controlling segmentation. This pattern of expression seems to be conserved in short- and intermediate-germ band embryogenesis as similar *FTZ-F1* expression in pair-rule stripes has been observed also in the beetles *Dermestes maculatus* and *T. castaneum*,<sup>48,49</sup> suggesting a conserved role of *FTZ-F1* in segmentation. In fact, functional studies in *T. castaneum* revealed that the depletion of *Tc-FTZ-F1* resulted in clear pair-rule segmentation defects.<sup>48,50</sup> Interestingly, the pair-rule function of *FTZ-F1* is conserved in the embryogenesis of long-germ band *D. melanogaster*, although in the fruit fly this factor is expressed ubiquitously in the embryo.<sup>51</sup> In this case, segment specification was achieved simultaneously by the interaction of ubiquitous *FTZ-F1* with the homeodomain protein Fushi Tarazu (*Ftz*), which was expressed in pair-rule stripes.<sup>52-54</sup> In this regard, it is interesting to note that *E75A*, another member of the cascade, exerts pair-rule functions in *O. fasciatus*,<sup>44</sup> suggesting that a combination of ecdysone-dependent nuclear receptors might be involved in the control of the segmentation process in short-germ band insects. Unfortunately, no embryonic functions for *E75A* have been characterized in any other short-germ band insect. In our case, we were not able to obtain a reliable depletion of embryonic *BgE75A* by pRNAi, probably due to the small size of the isoform-specific region (data not shown). It would be interesting in the future, then, to determine to what extent ecdysone-dependent nuclear receptors are involved in the control of segmentation to ascertain the ancestral functions of these genes in embryogenesis.

Finally, we have demonstrated a critical contribution of *BgFTZ-F1* in the oogenesis of adult *B. germanica* females. *BgFtz-F1* is expressed throughout the ovary during the whole gonadotrophic cycle, and its depletion results in the complete block of oogenesis due, at least in part, to failure in the reorganization of the actin filaments of the follicle cells during choriogenesis. Interestingly, *FTZ-F1* is also required for completing oogenesis in *T. castaneum*<sup>50</sup> and *D. melanogaster*.<sup>55,56</sup> In the fly, like in *B. germanica*, this factor is detected throughout the ovary and is required for follicle cells to differentiate properly into the final maturation stage.<sup>55,56</sup> Likewise, the mammalian *FTZ-F1* homolog, steroidogenic factor-1 (*SF-1*) has been also detected in somatic follicle cells in rodents and humans,<sup>57,58</sup> and its depletion in mouse granulosa cells results in the loss of developing follicles.<sup>59</sup> Together, these results highlight the conservation of the critical role of *FTZ-F1/SF-1* in the control of oogenesis in insects and mammals.

In summary, our work shows the pivotal role of ecdysone signaling during early embryogenesis in the hemimetabolous *B. germanica*, and identifies the formation and development of the germband as the first developmental transition in a short-germ band type of embryogenesis that depends on the ecdysone receptor. We can conclude, therefore, that in short-germ band hemimetabolous insects, ecdysone signaling acts as a central regulator of developmental transitions in embryonic and post-embryonic periods. However, given that some holometabolous species also undergo short-germ band embryonic development, further research using different short-germ band holometabolous species, would be required to ascertain the early presence of ecdysone signaling and to generalize the regulatory role of this pathway in this type of embryonic development. Finally, it is worth noting that our results show that ecdysone-signaling is required much earlier in short-germ band hemimetabolous than in long-germ band holometabolous embryogenesis, which raises the possibility that the loss of ecdysone-signaling during the initial stages of embryogenesis could be a key feature in the evolution of the different types of insect development.

### Limitations of the study

An efficient way to analyze gene function during embryogenesis by *in vivo* RNAi entails the microinjection of *dsRNAs* into eggs during the onset of embryonic development (from oviposition to the preblastoderm stage). However, the particular reproductive system of the cockroach *B. germanica*, which includes the encapsulation of fertilized eggs into a hard case, the ootheca, that will remain attached to the female until egg hatching, precludes the use of early eggs for injection. To circumvent this problem, we injected the *dsRNAs* into adult females at the end of their vitellogenic cycle, thus allowing for the incorporation of these *dsRNAs* into growing oocytes, thus allowing to analyze the lack of function of the target genes from the beginning of embryogenesis. However, the main limitation to this strategy is that interference of genes that are necessary for the correct completion of oogenesis and/or ovulation may result in females that do not form any ootheca, thus precluding the functional analysis of the embryonic role of these genes. Unfortunately, this has been the case of the nuclear receptor *BgFTZ-F1*, which ultimately prevented us from

testing whether this factor is involved in the control of segmentation during germband extension, as its embryonic expression pattern strongly suggested.

## STAR★METHODS

Detailed methods are provided in the online version of this paper and include the following:

- KEY RESOURCES TABLE
- RESOURCE AVAILABILITY
  - Lead contact
  - Materials availability
  - Data and code availability
- EXPERIMENTAL MODEL AND SUBJECT DETAILS
  - Insects
- METHODS DETAILS
  - Semiquantitative reverse transcriptase polymerase chain reaction (RT-PCR)
  - Quantitative real-time reverse transcriptase polymerase chain reaction (qRT-PCR)
  - Whole-mount hybridization *in situ*
  - Microscopy and histological analysis
  - Gene knockdown by parental RNA interference (pRNAi)
  - Quantification of embryonic ecdysteroid titers
- QUANTIFICATION AND STATISTICAL ANALYSIS
  - Statistical analysis

## SUPPLEMENTAL INFORMATION

Supplemental information can be found online at <https://doi.org/10.1016/j.isci.2023.106548>.

## ACKNOWLEDGMENTS

Support for this research was provided by grants CGL2014-55786-P and PGC2018-098427-B-I00 funded by MCIN/AEI/10.13039/501100011033 and by “ERDF A way of making Europe” to D.M. and X.F.-M. and by the Ministry of Research and Universities from the Catalan Government (2014 SGR 619 to D.M. and X.F.-M.).

## AUTHOR CONTRIBUTIONS

Conception and design of the project were done by J.C. and D.M. J.C. and O.M. performed the experiments. The analysis of the data was conducted by J.C. O.M. X.F.-M. and D.M. D.M. wrote the article and J.C. and X.F.-M. revised the article. All authors approved the final article.

## DECLARATION OF INTERESTS

The authors declare no competing interests.

Received: November 2, 2022

Revised: November 28, 2022

Accepted: March 27, 2023

Published: March 31, 2023

## REFERENCES

1. Rewitz, K.F., Yamanaka, N., and O'Connor, M.B. (2013). Developmental checkpoints and feedback circuits time insect maturation. *Curr. Top. Dev. Biol.* *103*, 1–33. <https://doi.org/10.1016/B978-0-12-385979-2.00001-0>.
2. Truman, J.W. (2019). The evolution of insect metamorphosis. *Curr. Biol.* *29*, R1252–R1268. <https://doi.org/10.1016/j.cub.2019.10.009>.
3. Henrich, V.C. (2012). The ecdysteroid receptor. In *Insect Endocrinology* (Salt Lake City, UT: Academic Press), pp. 177–218. <https://doi.org/10.1016/B978-0-12-384749-2.10005-6>.
4. Riddiford, L.M., Cherbas, P., and Truman, J.W. (2000). Ecdysone receptors and their biological actions. *Vitam. Horm.* *60*, 1–73. [https://doi.org/10.1016/S0083-6729\(00\)60016-X](https://doi.org/10.1016/S0083-6729(00)60016-X).
5. Yao, T.P., Segreaves, W.A., Oro, A.E., McKeown, M., and Evans, R.M. (1992). *Drosophila* ultraspiracle modulates ecdysone receptor function via heterodimer formation. *Cell* *71*, 63–72. [https://doi.org/10.1016/0092-8674\(92\)90266-F](https://doi.org/10.1016/0092-8674(92)90266-F).
6. Yao, T.P., Forman, B.M., Jiang, Z., Cherbas, L., Chen, J.D., McKeown, M., Cherbas, P., and Evans, R.M. (1993). Functional ecdysone receptor is the product of EcR and Ultraspiracle genes. *Nature* *366*, 476–479. <https://doi.org/10.1038/366476a0>.
7. Thomas, H.E., Stunnenberg, H.G., and Stewart, A.F. (1993). Heterodimerization of the *Drosophila* ecdysone receptor with

- retinoid X receptor and ultraspiracle. *Nature* 362, 471–475. <https://doi.org/10.1038/362471a0>.
8. Thummel, C.S. (1995). From embryogenesis to metamorphosis: the regulation and function of drosophila nuclear receptor superfamily members. *Cell* 83, 871–877. [https://doi.org/10.1016/0092-8674\(95\)90203-1](https://doi.org/10.1016/0092-8674(95)90203-1).
  9. Ou, Q., and King-Jones, K. (2013). What goes up must come down. Transcription factors have their say in making ecdysone pulses. *Curr. Top. Dev. Biol.* 103, 35–71. <https://doi.org/10.1016/B978-0-12-385979-2.00002-2>.
  10. Martín, D. (2010). Functions of Nuclear Receptors in Insect Development. [https://doi.org/10.1007/978-90-481-3303-1\\_3](https://doi.org/10.1007/978-90-481-3303-1_3).
  11. Cheatle Jarvela, A.M., and Pick, L. (2017). The function and evolution of nuclear receptors in insect embryonic development. *Curr. Top. Dev. Biol.* 39–70. <https://doi.org/10.1016/bs.ctdb.2017.01.003>.
  12. King-Jones, K., and Thummel, C.S. (2005). Nuclear receptors - a perspective from *Drosophila*. *Nat. Rev. Genet.* 6, 311–323. <https://doi.org/10.1038/nrg1581>.
  13. Davis, G.K., and Patel, N.H. (2002). Short, long, and beyond: molecular and embryological approaches to insect segmentation. *Annu. Rev. Entomol.* 47, 669–699. <https://doi.org/10.1146/annurev.ento.47.091201.145251>.
  14. Maróy, P., Kaufmann, G., and Dübendorfer, A. (1988). Embryonic ecdysteroids of *Drosophila melanogaster*. *J. Insect Physiol.* 34, 633–637. [https://doi.org/10.1016/0022-1910\(88\)90071-6](https://doi.org/10.1016/0022-1910(88)90071-6).
  15. Kraminsky, G.P., Clark, W.C., Estelle, M.A., Gietz, R.D., Sage, B.A., O'Connor, J.D., and Hodgetts, R.B. (1980). Induction of translatable mRNA for dopa decarboxylase in *Drosophila*: an early response to ecdysterone. *Proc. Natl. Acad. Sci. USA* 77, 4175–4179. <https://doi.org/10.1073/pnas.77.7.4175>.
  16. Kozlova, T., and Thummel, C.S. (2003). Essential roles for ecdysone signaling during *Drosophila* mid-embryonic development. *Science* 301, 1911–1914. <https://doi.org/10.1126/science.1087419>.
  17. Chavoshi, T.M., Moussian, B., and Uv, A. (2010). Tissue-autonomous EcR functions are required for concurrent organ morphogenesis in the *Drosophila* embryo. *Mech. Dev.* 127, 308–319. <https://doi.org/10.1016/j.mod.2010.01.003>.
  18. Ruard, A.F., Lam, G., and Thummel, C.S. (2010). The *Drosophila* nuclear receptors DHR3 and  $\beta$ FTZ-F1 control overlapping developmental responses in late embryos. *Development* 137, 123–131. <https://doi.org/10.1242/dev.042036>.
  19. Konopová, B., and Zrzavý, J. (2005). Ultrastructure, development, and homology of insect embryonic cuticles. *J. Morphol.* 264, 339–362. <https://doi.org/10.1002/jmor.10338>.
  20. Piulachs, M.D., Pagone, V., and Bellés, X. (2010). Key roles of the Broad-Complex gene in insect embryogenesis. *Insect Biochem. Mol. Biol.* 40, 468–475. <https://doi.org/10.1016/j.ibmb.2010.04.006>.
  21. Tanaka, A. (1976). *Stages in the Embryonic Development of the German Cockroach Blattella Germanica Linné (Blattaria, Blattellidae)*, 44 (Kontyu, Tokyo: The Entomological Society of Japan), pp. 512–525.
  22. Maestro, O., Cruz, J., Pascual, N., Martín, D., and Bellés, X. (2005). Differential expression of two RXR/ultraspiracle isoforms during the life cycle of the hemimetabolous insect *Blattella germanica* (Dictyoptera, Blattellidae). *Mol. Cell. Endocrinol.* 238, 27–37. <https://doi.org/10.1016/j.mce.2005.04.004>.
  23. Mané-Padrós, D., Cruz, J., Vilaplana, L., Pascual, N., Bellés, X., and Martín, D. (2008). The nuclear hormone receptor BgE75 links molting and developmental progression in the direct-developing insect *Blattella germanica*. *Dev. Biol.* 315, 147–160. <https://doi.org/10.1016/j.ydbio.2007.12.015>.
  24. Cruz, J., Mané-Padrós, D., Bellés, X., and Martín, D. (2006). Functions of the ecdysone receptor isoform-A in the hemimetabolous insect *Blattella germanica* revealed by systemic RNAi in vivo. *Dev. Biol.* 297, 158–171. <https://doi.org/10.1016/j.ydbio.2006.06.048>.
  25. Martín, D., Maestro, O., Cruz, J., Mané-Padrós, D., and Bellés, X. (2006). RNAi studies reveal a conserved role for RXR in molting in the cockroach *Blattella germanica*. *J. Insect Physiol.* 52, 410–416. <https://doi.org/10.1016/j.jinsphys.2005.12.002>.
  26. Cruz, J., Martín, D., and Bellés, X. (2007). Redundant ecdysis regulatory functions of three nuclear receptor HR3 isoforms in the direct-developing insect *Blattella germanica*. *Mech. Dev.* 124, 180–189. <https://doi.org/10.1016/j.mod.2006.12.003>.
  27. Cruz, J., Nieva, C., Mané-Padrós, D., Martín, D., and Bellés, X. (2008). Nuclear receptor BgFTZ-F1 regulates molting and the timing of ecdysteroid production during nymphal development in the hemimetabolous insect *Blattella germanica*. *Dev. Dyn.* 237, 3179–3191. <https://doi.org/10.1002/dvdy.21728>.
  28. Mané-Padrós, D., Cruz, J., Vilaplana, L., Nieva, C., Ureña, E., Bellés, X., and Martín, D. (2010). The hormonal pathway controlling cell death during metamorphosis in a hemimetabolous insect. *Dev. Biol.* 346, 150–160.
  29. Mané-Padrós, D., Borrás-Castells, F., Bellés, X., and Martín, D. (2012). Nuclear receptor HR4 plays an essential role in the ecdysteroid-triggered gene cascade in the development of the hemimetabolous insect *Blattella germanica*. *Mol. Cell. Endocrinol.* 348, 322–330. <https://doi.org/10.1016/j.mce.2011.09.025>.
  30. Ylla, G., Piulachs, M.D., and Bellés, X. (2018). Comparative transcriptomics in two extreme neopterans reveals general trends in the evolution of modern insects. *iScience* 4, 164–179. <https://doi.org/10.1016/j.isci.2018.05.017>.
  31. Sonobe, H., and Yamada, R. (2004). Ecdysteroids during early embryonic development in silkworm *Bombyx mori*: metabolism and functions. *Zool. Sci.* 21, 503–516. <https://doi.org/10.2108/zsj.21.503>.
  32. Makka, T., and Sonobe, H. (2000). Ecdysone metabolism in diapause eggs and non-diapause eggs of the silkworm, *Bombyx mori*. *Zool. Sci.* 17, 89–95. <https://doi.org/10.2108/zsj.17.89>.
  33. Horike, N., and Sonobe, H. (1999). Ecdysone 20-monooxygenase in eggs of the silkworm, *Bombyx mori*: enzymatic properties and developmental changes. *Arch. Insect Biochem. Physiol.* 41, 9–17. [https://doi.org/10.1002/\(SICI\)1520-6327](https://doi.org/10.1002/(SICI)1520-6327).
  34. Schöck, F., and Perrimon, N. (2002). Cellular processes associated with germ band retraction in *Drosophila*. *Dev. Biol.* 248, 29–39. <https://doi.org/10.1006/dbio.2002.0698>.
  35. Bownes, M., Shirras, A., Blair, M., Collins, J., and Coulson, A. (1988). Evidence that insect embryogenesis is regulated by ecdysteroids released from yolk proteins. *Proc. Natl. Acad. Sci. USA* 85, 1554–1557. <https://doi.org/10.1073/pnas.85.5.1554>.
  36. Lanzrein, B., Gentinetta, V., Abegglen, H., Baker, F.C., Miller, C.A., and Schooley, D.A. (1985). Titters of ecdysone, 20-hydroxyecdysone and juvenile hormone III throughout the life cycle of a hemimetabolous insect, the ovoviparous cockroach *Nauphoeta cinerea*. *Experientia* 41, 913–917. <https://doi.org/10.1007/BF01970010>.
  37. Bullière, D., Bullière, F., and de Reggi, M. (1979). Ecdysteroid titres during ovarian and embryonic development in *Blaberus craniifer*. *Wilhelm Roux's Arch. Dev. Biol.* 186, 103–114. <https://doi.org/10.1007/BF00848172>.
  38. Lagueux, M., Hetru, C., Goltzene, F., Kappler, C., and Hoffmann, J.A. (1979). Ecdysone titre and metabolism in relation to cuticulogenesis in embryos of *Locusta migratoria*. *J. Insect Physiol.* 25, 709–723. [https://doi.org/10.1016/0022-1910\(79\)90123-9](https://doi.org/10.1016/0022-1910(79)90123-9).
  39. Sullivan, A.A., and Thummel, C.S. (2003). Temporal profiles of nuclear receptor gene expression reveal coordinate transcriptional responses during *Drosophila* development. *Mol. Endocrinol.* 17, 2125–2137. <https://doi.org/10.1210/me.2002-0430>.
  40. Yamada, R., and Sonobe, H. (2003). Purification, kinetic characterization, and molecular cloning of a novel enzyme ecdysteroid-phosphate phosphatase. *J. Biol. Chem.* 278, 26365–26373. <https://doi.org/10.1074/jbc.M304158200>.
  41. Herboso, L., Oliveira, M.M., Talamillo, A., Pérez, C., González, M., Martín, D., Sutherland, J.D., Shingleton, A.W., Mirth, C.K., and Barrio, R. (2015). Ecdysone promotes growth of imaginal discs through the regulation of Thor in *D. melanogaster*.



- Sci. Rep. 5, 12383. <https://doi.org/10.1038/srep12383>.
42. Verma, P., and Cohen, S.M. (2015). miR-965 controls cell proliferation and migration during tissue morphogenesis in the *Drosophila* abdomen. *Elife* 4, e07389. <https://doi.org/10.7554/elife.07389>.
43. Ninov, N., Manjón, C., and Martín-Blanco, E. (2009). Dynamic control of cell cycle and growth coupling by ecdysone, *egfr*, and PI3K signaling in *Drosophila* histoblasts. *PLoS Biol.* 7, 0892–0903. <https://doi.org/10.1371/journal.pbio.1000079>.
44. Erezylmaz, D.F., Kelstrup, H.C., and Riddiford, L.M. (2009). The nuclear receptor E75A has a novel pair-rule-like function in patterning the milkweed bug, *Oncopeltus fasciatus*. *Dev. Biol.* 334, 300–310. <https://doi.org/10.1016/j.ydbio.2009.06.038>.
45. SurrIDGE, A.K., Lopez-Gomollon, S., Moxon, S., Maroja, L.S., Rathjen, T., Nadeau, N.J., Dalmay, T., and Jiggins, C.D. (2011). Characterisation and expression of microRNAs in developing wings of the neotropical butterfly *Heliconius melpomene*. *BMC Genom.* 12, 62. <https://doi.org/10.1186/1471-2164-12-61>.
46. Schröder, R. (2003). The genes *orthodenticle* and *hunchback* substitute for *bicoid* in the beetle *Tribolium*. *Nature* 422, 621–625. <https://doi.org/10.1038/nature01536>.
47. Nakamura, T., Yoshizaki, M., Ogawa, S., Okamoto, H., Shinmyo, Y., Bando, T., Ohuchi, H., Noji, S., and Mito, T. (2010). Imaging of transgenic cricket embryos reveals cell movements consistent with a syncytial patterning mechanism. *Curr. Biol.* 20, 1641–1647. <https://doi.org/10.1016/j.cub.2010.07.044>.
48. Heffer, A., Grubbs, N., Mahaffey, J., and Pick, L. (2013). The evolving role of the orphan nuclear receptor *ftz-f1*, a pair-rule segmentation gene. *Evol. Dev.* 15, 406–417. <https://doi.org/10.1111/ede.12050>.
49. Xiang, J., Reding, K., Heffer, A., and Pick, L. (2017). Conservation and variation in pair-rule gene expression and function in the intermediate-germ beetle *Dermestes maculatus*. *Development (Camb.)* 144, 4625–4636. <https://doi.org/10.1242/dev.154039>.
50. Xu, J., Tan, A., and Palli, S.R. (2010). The function of nuclear receptors in regulation of female reproduction and embryogenesis in the red flour beetle, *Tribolium castaneum*. *J. Insect Physiol.* 56, 1471–1480. <https://doi.org/10.1016/j.jinsphys.2010.04.004>.
51. Yussa, M., Löhr, U., Su, K., and Pick, L. (2001). The nuclear receptor Ftz-F1 and homeodomain protein Ftz interact through evolutionarily conserved protein domains. *Mech. Dev.* 107, 39–53. [https://doi.org/10.1016/S0925-4773\(01\)00448-8](https://doi.org/10.1016/S0925-4773(01)00448-8).
52. Yu, Y., Li, W., Su, K., Yussa, M., Han, W., Perrimon, N., and Pick, L. (1997). The nuclear hormone receptor Ftz-F1 is a cofactor for the *Drosophila* homeodomain protein Ftz. *Nature* 385, 552–555. <https://doi.org/10.1038/385552a0>.
53. Florence, B., Guichet, A., Ephrussi, A., and Laughon, A. (1997). Ftz-F1 is a cofactor in Ftz activation of the *Drosophila* engrailed gene. *Development* 124, 839–847. <https://doi.org/10.1242/dev.124.4.839>.
54. Guichet, A., Copeland, J.W., Erdélyi, M., Hlousek, D., Závorszky, P., Ho, J., Brown, S., Percival-Smith, A., Krause, H.M., and Ephrussi, A. (1997). The nuclear receptor homologue Ftz-F1 and the homeodomain protein Ftz are mutually dependent cofactors. *Nature* 385, 548–552. <https://doi.org/10.1038/385548a0>.
55. Beachum, A.N., Whitehead, K.M., McDonald, S.I., Phipps, D.N., Berghout, H.E., and Ables, E.T. (2021). Orphan nuclear receptor *ftz-f1* (NR5A3) promotes egg chamber survival in the *Drosophila* ovary. *G3* 11, jkab003. <https://doi.org/10.1093/g3journal/jkab003>.
56. Knapp, E.M., Li, W., Singh, V., and Sun, J. (2020). Nuclear receptor *ftz-f1* promotes follicle maturation and ovulation partly via *bhlh/pas* transcription factor *sim*. *Elife* 9, e54568. <https://doi.org/10.7554/eLife.54568>.
57. Tajima, K., Dantes, A., Yao, Z., Sorokina, K., Kotsuji, F., Seger, R., and Amsterdam, A. (2003). Down-regulation of steroidogenic response to gonadotropins in human and rat preovulatory granulosa cells involves mitogen-activated protein kinase activation and modulation of DAX-1 and steroidogenic factor-1. *J. Clin. Endocrinol. Metab.* 88, 2288–2299. <https://doi.org/10.1210/jc.2002-020913>.
58. Hinshelwood, M.M., Repa, J.J., Shelton, J.M., Richardson, J.A., Mangelsdorf, D.J., and Mendelson, C.R. (2003). Expression of LRH-1 and SF-1 in the mouse ovary: localization in different cell types correlates with differing function. *Mol. Cell. Endocrinol.* 207, 39–45. [https://doi.org/10.1016/S0303-7207\(03\)00257-0](https://doi.org/10.1016/S0303-7207(03)00257-0).
59. Pelusi, C., Ikeda, Y., Zubair, M., and Parker, K.L. (2008). Impaired follicle development and infertility in female mice lacking steroidogenic factor 1 in ovarian granulosa cells. *Biol. Reprod.* 79, 1074–1083. <https://doi.org/10.1095/biolreprod.108.069435>.

## STAR★METHODS

### KEY RESOURCES TABLE

REAGENT or RESOURCE	SOURCE	IDENTIFIER
<b>Antibodies</b>		
Mouse anti-engrailed/injected 4D9	Abcam	Cat#:12454; RRID:AB_528224
Rabbit anti-phospho-Histone H3	Cell Signalling	Cat#:9701S; RRID:AB_331535
Rabbit anti-cleaved dcp-1	Cell Signalling	Cat#:9578S; RRID:AB_2721060
Anti-mouse IgG-peroxidase	Merck	Cat#:A2304
Anti-rabbit IgG-peroxidase	Merck	Cat#:A6154
Anti-digoxin-AP Fab fragments	Merck	Cat#:11093274910; RRID:AB_514497
<b>Chemicals, peptides, and recombinant proteins</b>		
NBT/BCIP Stock Solution	Merck	Cat#:11681451001
Paraformaldehyde	Merck	Cat#:76240
Ethanol	Carlo-Erba reagents	Cat#:4146072
Deionized formamide	Fluka	Cat#:47670
iTaq Universal SYBR Green Supermix	BioRad	Cat#:1725121
SP6 RNA polymerase	Roche	Cat#:P1085
T7 RNA polymerase	Roche	Cat#:P2075
Bovine Serum Albumin	Merck	Cat#:A2153
Vectashield medium with DAPI	Vector Laboratories	Cat#:H1200
Triton X-100	United States Biochemical	Cat#:22686
Tween-20	Merck	Cat#:P9416
RQ1 DNase	Promega	Cat#:M298A
2-mercaptoethanol	Merck	Cat#:M3148
Methanol	Carlo Erba Reagents	Cat#:414814
normal goat serum	Fisher Scientific	Cat#:PCN5000
Ribonucleic acid transfer from Baker's yeast	Merck	Cat#:R5636
Deoxyribonucleic acid sodium salt from salmon testes	Merck	Cat#:D1626
Proteinase K	Merck	Cat#:3115887001
phalloidin-TRITC	Merck	Cat#:P1951
Heparin sodium salt from, porcine intestinal mucosa	Merck	Cat#:H3393
<b>Critical commercial assays</b>		
GeneElute™ Mammalian Total RNA kit.	Merck	Cat#: RTN70
20-Hydroxycyclopropane ELISA Kit	Bertin Bioreagents	Cat#:A05120
Transcription First Strand cDNA Synthesis Kit	Roche	Cat#:04379012001
DIG RNA Labeling Mix	Roche	Cat#:11277073
<b>Oligonucleotides</b>		
See Table S3	N/A	N/A
<b>Software and algorithms</b>		
GraphPad Prism v4.00 software	GraphPad Software Inc.	RRID: SCR_002285
Photoshop CS4	Adobe Inc.	<a href="https://www.adobe.com">https://www.adobe.com</a>
iCycler iQ Real Time PCR Detection System	Bio-Rad	<a href="https://www.bio-rad.com/">https://www.bio-rad.com/</a>
Microsoft Excel	Microsoft	02992-000-000010

## RESOURCE AVAILABILITY

### Lead contact

Further information and requests for resources and reagents should be directed to and will be fulfilled by the lead contact, Josefa Cruz ([josefa.cruz@ibe.upf-csic.es](mailto:josefa.cruz@ibe.upf-csic.es)).

### Materials availability

This study did not generate new unique reagents.

### Data and code availability

This paper does not report original code.

## EXPERIMENTAL MODEL AND SUBJECT DETAILS

### Insects

Specimens of *B. germanica* were obtained from a colony reared in the dark at  $30 \pm 1^\circ\text{C}$  and 60–70% r.h. Under our rearing conditions, embryogenesis in *B. germanica* lasts 17 days, during which eggs developed within an ootheca that was carried by the female. All dissection and tissue sampling were carried out in Ringer's saline using carbon dioxide-anesthetized specimens.

## METHODS DETAILS

### Semiquantitative reverse transcriptase polymerase chain reaction (RT-PCR)

RT-PCR followed by southern blotting with specific probes was used to determine the embryonic and ovarian expression pattern of genes involved in the research. For the spatial analysis of *BgFTZ-F1* expression in adult ovaries, different parts of 7 day-old-female ovaries were separated by manual dissection. The different analyzed parts were: whole ovariole, ovariole without basal oocyte, basal oocyte, basal oocyte without surrounding follicle cells, and isolated follicle cells. Total RNA was extracted from embryos and ovaries using the GeneElute Mammalian Total RNA kit (Merck). cDNA synthesis was carried out as previously described.<sup>24</sup> Primers for the amplification of the corresponding genes can be found at [Table S3](#). As a reference the same cDNAs were subjected to RT-PCR with a primer pair specific for *B. germanica Actin5C*. cDNA samples were subjected to PCR with a number of cycles within the linear range of amplification for each transcript depending on the tissue and physiological stage.

### Quantitative real-time reverse transcriptase polymerase chain reaction (qRT-PCR)

Total RNA extraction and cDNA synthesis was carried out as described above. Relative transcripts levels were determined by quantitative real-time PCR (qPCR), using iQ SYBR Green supermix (Bio-Rad), and forward and reverse primers (final concentration: 100nM/qPCR) in a 20  $\mu\text{l}$  final volume (see [Table S3](#) for primer sequences). The qPCR experiments were conducted with the same quantity of embryo equivalent input for all treatments and each sample was run in duplicate using 2  $\mu\text{l}$  of cDNA per reaction. All the samples were analyzed using an iCycler and iQ Real Time PCR Detection System (Bio-Rad). For each standard curve, one reference DNA sample was diluted serially. RNA expression was normalized in relation to the expression of *BgActin-5C*.

### Whole-mount hybridization *in situ*

Digoxigenin-labeled RNA probes (sense and antisense) were generated by transcription *in vitro* using SP6 or T7 RNA polymerases (Roche) as previously described.<sup>24</sup> For *BgEcR-A* and *BgHR3-A* probes, 527-bp and 520-bp fragments, respectively, containing the specific A/B domains were used. For *BgE75*, *BgFTZ-F1* and *BgRXR* probes, 487-bp, 542-bp and 497-bp fragments within their ligand binding domains were used. For hybridization *in situ*, tissues were dissected in Ringer's saline and fixed for 1 h with 4% paraformaldehyde in PBS. Tissues were washed in PBT (PBS; 0.2% Tween-20), treated with 40  $\mu\text{g}/\text{ml}$  Proteinase K for 10 min, washed for 5 min in 2 mg/ml glycine in PBT, washed for 5 min in PBT and refixed for 20 min. After additional washes with PBT, the tissues were prehybridized in HS solution (50% formamide;  $5\times$  SSC; 50  $\mu\text{g}/\text{ml}$  heparin; 0.1% Tween 20; 100  $\mu\text{g}/\text{ml}$  sonicated and denatured ssDNA; 100  $\mu\text{g}/\text{ml}$  tRNA from yeast) at  $56^\circ\text{C}$  for 2 h. After prehybridization, sense or antisense probes were added to the HS solution and incubated overnight at  $56^\circ\text{C}$ . Tissues were then successively washed in HS for 20 min, HS:PBTB/N (1:1) (0.2% Tween 20; 1% BSA; 10% inactivated normal goat serum in PBS) for 20 min and PBTB/N for 5 min. Samples were then blocked in PBTB/N for 2 h at room temperature. Tissues were incubated with the alkaline phosphatase-conjugated

anti-digoxigenin antibody (preabsorbed with tissues of interest before hybridization) diluted 1:1000 in PBTB/N overnight at 4°C. Finally, tissues were washed in PBT for 2 h and hybridization was detected with the DIG Nucleic Acid Detection Kit (Roche), according to the manufacturer's instructions. Samples were mounted in 90% glycerol in PBS and examined using a Zeiss Axiophot microscope.

### Microscopy and histological analysis

For immunocytochemistry, embryos were dissected and fixed in 4% paraformaldehyde-PEM (100 mM Pipes, 2 mM EGTA, 1 mM MgSO<sub>4</sub>), permeabilized in PBST (PBS, 0,1% Triton) and incubated overnight at 4°C with the primary antibody diluted in PBSTBN (PBST, 0,1% BSA, 5% NGS). The following primary antibodies were used at indicated dilution: mouse anti- engrailed/invented 4D9 (Abcam, 1:1), rabbit anti-phospho-Histone H3 (Ser10) (Cell Signalling, 1:1000) and rabbit anti-cleaved dcp-1 (Cell Signalling, 1:100). They were then washed with PBST and incubated with the secondary antibody: anti-mouse IgG-peroxidase (Merck, 1:100) or anti-rabbit IgG-peroxidase (Merck, 1:50) diluted in PBST for to 2 h and washed with PBST. The DAB reaction was performed for 3–5 min and embryos mounted for visualization in 50% glycerol in PBS. For fluorescent imaging, dissected ovaries were dissected in Ringer and fixed in 4% paraformaldehyde in PBS. Permeabilized in PBST and incubated for 20 min in a 300 ng/ml solution of phalloidin-TRITC in PBS. Rinsed with PBST and mounted in Vectashield medium with DAPI (Vector Laboratories, H1200). All samples were examined with a Zeiss Axiophot microscope, and images were subsequently processed using Adobe photoshop.

### Gene knockdown by parental RNA interference (pRNAi)

The primers used to generate templates via PCR for transcription of the dsRNAs are described in [Table S3](#). Synthesis of double-stranded RNA was performed as previously described.<sup>24</sup> A volume of 1 µl of each dsRNA solution (3–5 µg/µL) was injected into the abdomen of adult females. Under our rearing conditions, the first adult gonadotrophic cycle lasts seven days. During this period, only the basal oocyte of each ovariole matures and grows, whereas the remaining oocytes of the ovariole keep immature. When maturation is completed, basal oocytes form the chorion and are oviposited into an attached ootheca where embryogenesis takes place. To determine the optimal range of adult female age for pRNAi experiments, we injected dsRNAs into adult females from day 0 to day 7, and found that injection into 5-days-old females produced the best pRNAi effect for *BgEcR-A*, *BgRXR* and *BgHR3*. In the case of *BgFTZ-F1*, no oothecae were formed regardless of the female age at which the dsRNA was injected. For the analysis of the role of *BgFTZ-F1* in oogenesis, dsRNA for *BgFTZ-F1* was injected into newly ecdysed adult females. Control dsRNA (Control) consisted of a non-coding sequence from the pSTBlue-1 vector.

### Quantification of embryonic ecdysteroid titers

20 staged oothecas for each time point were preserved in 500ul of methanol, homogenized and centrifuged (10 min at 18000 x g). The remaining tissue was re-extracted twice in 0.5 mL methanol and the resulting methanol supernatants were dried using a SpeedVac. Samples were resuspended in enzyme immunoassay buffer (0.4 cM NaCl, 1cmM EDTA, 0.1% bovine serum albumin in 0.1 M phosphate buffer). ELISA was performed according to the manufacturer's instructions using a commercial ELISA kit (Bertin Bio-reagents) that detects ecdysone and 20-hydroxyecdysone with the same affinity. Absorbance was measured at 405 nm on a plate reader, SpectramaxPlus (Molecular Devices, Sunnyvale, CA) using GraphPad Prism v4.00 software (GraphPad Software Inc., San Diego, CA).

## QUANTIFICATION AND STATISTICAL ANALYSIS

### Statistical analysis

The analysis of gene knockdown phenotype by pRNAi were performed with 15 to 30 ootheca and the number of embryos analyzed is indicated in [Tables S1](#) and [S2](#). Blots in [Figures 2A](#), [S4A](#), [S4C](#), [S4D](#), [S5A](#), and [S5B](#) correspond to a representative of five to ten replicates. At qPCR analysis in [Figure 4](#) and at ecdysteroids measurement in [Figure S3B](#) each biological replicate corresponds to number of oothecas. Quantifications at graphs in [Figures 3B](#), [3D](#), and [3E](#) were performed in individual embryos. The number of biological replicates are indicated in the figure legends. Vertical bars in graphs of [Figures 3B](#), [3D](#), [3E](#), [4](#), and [3](#), correspond to SEM and a two-tailed Student's test was performed to determine which values were significantly different. Asterisks indicate differences statistically significant at  $p \leq 0.005$  (\*\*) and  $p \leq 0.0005$  (\*\*\*).